Solar Energy Materials & Solar Cells 116 (2013) 203–218

Contents lists available at SciVerse ScienceDirect

Solar Energy Materials & Solar Cells

journal homepage: www.elsevier.com/locate/solmat

Determining the degree of crosslinking of ethylene vinyl acetate photovoltaic module encapsulants—A comparative study

Ch. Hirschl [a,*], M. Biebl–Rydlo [a], M. DeBiasio [a], W. Mühleisen [a], L. Neumaier [a], W. Scherf [a], G. Oreski [b], G. Eder [c], B. Chernev [d], W. Schwab [e], M. Kraft [a]

[a] CTR Carinthian Tech Research AG, Europastraße 4/1, 9524 Villach, Austria
[b] PCCL Polymer Competence Center Leoben, Roseggerstraße 12, 8700 Leoben
[c] OFI Österreichisches Forschungsinstitut für Chemie und Technik, Arsenal Objekt 213, Franz-Grill-Straße 5, 1030 Wien, Austria
[d] Austrian Centre for Electron Microscopy and Nanoanalysis Graz and Research Institute for Electron Microscopy and Fine Structure Research, Steyrergasse 17/III, 8010 Graz, Austria
[e] ZT Büro Werner Schwab, Hammergasse 6, 9500 Villach, Austria

ARTICLE INFO

Article history:
Received 20 December 2012
Received in revised form
22 March 2013
Accepted 20 April 2013
Available online 6 June 2013

Keywords:
Ethylene vinyl acetate
Degree of crosslinking
Analytical method
Comparative study

ABSTRACT

A total of 16 analytical methods, spanning from classical solvent extraction over different thermo-analytic and mechanical approaches to acoustic and optical spectroscopy, have been evaluated as to their ability to determine the crosslinking state of ethylene vinyl acetate (EVA), the prevailing encapsulant for photovoltaics applications. The key objective of this work was to create a systematic and comprehensive comparison, using a unified set of traceable test samples covering the full range of realistically occurring degrees of EVA crosslinking. A majority number of these tested methods proved fundamentally suitable for detecting changes in the polymer properties during crosslinking based on the effect e.g. its mechanical properties or its crystallinity. Interestingly, when investigated in detail, most of the methods showed mutually different dependencies on the lamination time, indicating a complex range of effects of the chemical crosslinking on the properties and behaviour of the material. Furthermore, Raman spectroscopy could be identified as a potential new method for measuring the degree of crosslinking in-line in the PV module manufacturing process, thus providing an interesting approach for improving process control in PV module processing.

1. Introduction

With the rampant use of photovoltaic (PV) installations in both large-scale solar plants and house-top sites, increasing attention is given to their reliability and long-term performance over – expected – periods of use of up to 30 years. To be competitive in the market, PV module manufactures now (have to) warrant operational lifetimes of at least 20 years over which the total yield loss may not exceed 20% [1]. This resulted in a renewed interest in installing high-level quality assurance systems in PV module manufactories. Accordingly, a range of off-line and in-line control and analysis methods are being offered for examining both the single PV module components coming into and the assembled PV modules leaving the production line. While providing reliable information on the state of the modules directly after production, which is of both technical and commercial interest, very little information regarding the expectable long-term performance of the modules can be gained from this data [2].

When examining standard PV modules, one component known to be prone to aging, and hence likely to critically influence the long-term characteristics, is the solar cell encapsulant. Regardless of the chosen materials and the structural build-up of the PV module, the encapsulant has to fulfil several basic functions: firstly, it connects the components and provides structural support and mechanical protection to the solar cells, preventing over-stressing and cell cracking [3]. This includes dealing with the different thermal expansion of the various materials used in a PV module, i.e. glass, polymers, solar cells and interconnects [4]. Simultaneously, the encapsulant has to maintain electrical insulation and prevent the ingression of ambient media (humidity, etc.). Finally, it is essential to provide an optimal optical coupling (initial transmission≥90%) between the incident solar irradiation and the

* Corresponding author. Tel.: +43 4242 56300 238; fax: +43 4242 56300 400.
E-mail addresses: christina.hirschl@ctr.at (Ch. Hirschl), medea.bieblrydlo@ctr.at (M. Biebl–Rydlo), martin.debiasio@ctr.at (M. DeBiasio), wolfgang.muehleisen@ctr.at (W. Mühleisen), lukas.neumaier@ctr.at (L. Neumaier), werner.scherf@ctr.at (W. Scherf), gernot.oreski@pccl.at (G. Oreski), gabriele.eder@ofi.at (G. Eder), boril.chernev@felmi-zfe.at (B. Chernev), w.schwab@acoustics.at (W. Schwab), martin.kraft@ctr.at (M. Kraft).

http://dx.doi.org/10.1016/j.solmat.2013.04.022
0927-0248/

solar cells in the relevant spectral region. All these functions have to be maintained over the entire operational lifetime of the module; for instance, the loss in light transmission deemed acceptable is less than 5% over 20 years [1]. Thus, the general characteristics of PV encapsulation materials are very similar: optically transparent, electrically insulating and soft but dimensionally stable, with good adhesion properties and lasting aging resistance—all at possibly low cost. While a range of materials have been described for this purpose, and new ideas and concepts are constantly being introduced, up to now the by far dominating encapsulation material for PV modules is crosslinked ethylene vinyl acetate (EVA).

EVA in general is a random copolymer of ethylene and vinyl acetate; for PV applications, the percentage of vinyl acetate is typically in the range 28–33% (w/w). Thermoplastic, with a melting range of 60–70 °C, mildly opaque, soft and easily plastically deformable, this native EVA material would fulfil neither the mechanical nor the optical requirements. However, by crosslinking the copolymer chains during module lamination, the mouldable EVA sheet is transformed into an elastomeric, highly transparent encapsulation. The underlying process is the formation of a loose 3-dimensional polymer network, thus increasing the mechanical and thermal stability of the then elastomeric material. Crosslinking EVA is only feasible via a radical reaction, using an organic peroxide or peroxycarboxylic acid as radical initiator ("crosslinker") [1]. Initially, this crosslinker is homolytically cleaved into two radical species, which then abstract hydrogen from the EVA chains, preferably from terminal methyl groups of the vinyl acetate sidechains. In this process, the active radical site is transferred to the methyl group, which then reacts with another active site in its vicinity, creating a chemical bond between the polymer chains and transforming the initially thermoplastic EVA into a "cured" three-dimensionally crosslinked elastomer [5]. In PV module manufacturing, this radical reaction is prevalently thermally activated, i.e. the homolytic cleavage is the result of a thermal decomposition ("thermolysis") of the radical crosslinker at typically ~150 °C during lamination. While the following crosslinking process comprises a myriad of possible radical reactions, many of which are unknown in detail, these are significantly faster than the initial homolytic thermolysis of the crosslinker. In combination with a vast excess of polymer over the amount of crosslinker present, this yields approximately (pseudo-)first order reaction kinetics of the crosslinking [6] with a rate constant controlled mainly by the cleavage reaction of the initiator. Assuming this reaction to follow the classical Arrhenius law equation, for a given radical initiator chemistry the lamination temperature is the only variable parameter affecting the rate of crosslinking. The degree of crosslinking is thus controlled by (*i*) the *lamination temperature* (affecting the amount of crosslinker activated per time unit), (*ii*) the *lamination time* and (*iii*) the initial *crosslinker concentration*.

This chemical assessment of the crosslinking reaction kinetics has been validated in practice. Lange et al. have shown that the degree of crosslinking is indeed strongly affected by both lamination time and lamination temperature [7]. However, while controlling these two parameters is a requisite for high-quality module production, it is still insufficient to warrant sustainably high product quality, in particular over several decades of operational lifetime. At the same time, studies of the long-term characteristics of elastomers and their change over time have shown that these are strongly influenced by the initial degree of crosslinking [1]. This renders the degree of crosslinking of the EVA encapsulant – or other elastomeric encapsulation materials for PV applications – a key control parameter for PV module production. Given the increasing degree of automation, PV manufacturers would hence be very much interested in a reliable method for measuring the degree of encapsulant crosslinking, preferably in-line and in-situ, for use in process development and optimisation as well as in quality control.

In strong contrast to these demands, the standard method to measure the degree of EVA crosslinking is a Soxhlet–type extraction process [8], which determines the amount of non-linked and hence soluble/leachable polymer. While comparatively simple in design and procedure, this method has some fundamental disadvantages: first, with typical test durations > 24 h, the method is clearly off-line and hence limited to method development and post-production quality control, but hardly applicable for real-time process control. Secondly, the method requires sampling of the crosslinked EVA, which is hard to come by from an assembled PV module. Thirdly, the method cannot differentiate between singly and multiply crosslinked polymer chains; this number of bonds formed, however, is likely to strongly influence the thermo-mechanical properties of the encapsulant, and hence its long-term performance in use.

To overcome these issues, a number of alternative analysis methods based on thermal or mechanical principles have been investigated [9–15,17], but none of them could be established in the PV industry up to now. One reason for this is that all these methods require sampling and are hence destructive, making it impossible to use them for quality control of assembled PV modules. A second reason is a lack of a systematic evaluation and comprehensive comparison of the different approaches for measuring the degree of crosslinking of EVA encapsulation materials. Hence, the key objective of this paper was to evaluate and compare the various possible methods using a unified set of traceable EVA test samples covering the full range of realistically occurring degrees of crosslinking in a PV-module. The results were evaluated against the established standard and also against each other. Additionally, the findings were interpreted with respect to applicable chemical and physical fundamentals. In a final step, the methods were assessed as to their ability to provide reliable indicators describing the degree of EVA crosslinking and their potentials for future industrial (in-line) application.

2. Materials and methods

2.1. Unified test substrates

To provide a reliable basis for the subsequent evaluation and comparison, EVA test samples varying only in the degree of crosslinking was produced in a standardised process. The experimental design followed the industrial practice of controlling the degree of crosslinking mainly via the lamination time while keeping the lamination temperature and the composition of the EVA foil constant. Hence, the degree of crosslinking was varied solely by changing the duration of the lamination process.

The EVA used for the tests was a standard PV encapsulation material (Vistasolar® 486, SolutiaSolar GmbH). The lamination process itself was carried out in a manual laminator following standard lamination procedures. First, the panel components, i.e. two 150 × 100 cm² solar glasses, each covered with a fluorinated separating foil (FEP500C, DuPont), and a single 450 μm EVA sheet in between, were stacked manually. The fluorinated sheets were added to prevent adhesion of the cured EVA to the glass and allow recovering the test samples. These stacks were then placed in the pre-heated laminator, the lamination chamber evacuated for 4 min to raw vacuum levels and the module stack shifted to the heating plate. Upon contact, the chamber was evacuated to the final fine vacuum (60 Pa), followed by applying a pressure of ~85 kPa to the stack via a pressure plate. At that step, the stack made full contact with the heating plate, thus initiating the EVA crosslinking and starting the clock on the *lamination time*. For the purpose of this study, the lamination time was systematically varied from 0 to 10 min (with 7–8 min being the industrial

standard) in 2 min increments, with the lamination temperature kept constant at 150 °C. After the end of the set time, the laminator was vented, the panel removed and the EVA sample recovered. Thus, all samples experienced identical pre- and post-treatment in respect to temperature and pressure, the only variable being the actual crosslinking time.

Three independent test items a, b and c of each of the differently timed/crosslinked samples, subsequently denoted *S*0 to *S*10, were manufactured in non-sequential order following this standard procedure. The sheets were anonymised for the subsequent analyses using unique but arbitrary tracking codes, cut into pieces and identical samples provided for all comparative experiments.

Two of the chosen analytical approaches required deviations from this standard procedure. For the scanning acoustic microscopy investigations, each EVA test sheet was laminated onto a 34 × 34 cm² polyamide backsheet (ICOSOLAR® AAA 3554, Isovoltaic AG). For the laser scanning vibrometry tests, assembled PV test modules were created by laminating the EVA sheets between a 34 × 34 cm² standard solar glass (Petraglass GmbH) and a correspondingly sized polyamide backsheet (ICOSOLAR® AAA 3554, Isovoltaic AG).

2.2. Chemical methods

2.2.1. Soxhlet extraction method

With the Soxhlet test being the established "gold standard" used by most module manufacturers to control the lamination quality of EVA encapsulants for PV modules, the respective ASTM procedure [8] was strictly followed: first, three specimens, each weighing ~2 g, were cut from different sections of each EVA sample to be tested. The exact initial weight of each specimen (M_1) was determined on a precision balance. The specimen was then cut into 1 × 1 cm² pieces, put in a filter holder and refluxed for 8 h in a xylene isomer mixture (puriss. p.a., SigmaAldrich). After this treatment, the non-crosslinked fraction was supposed to be fully dissolved in the xylene and could be separated from the remaining, crosslinked and hence insoluble, elastomer matrix ("gel"). This insoluble residue was dried at 80 °C for 24 h, followed by the determination of its net weight (M_2). The ratio of the mass of the insoluble residue divided by the initial mass of the test sample yields the method's measurand "gel content":

$$\text{Gel Content } [\%] = \left(\frac{M_2}{M_1}\right)100, \quad M_2 \le M_1 \tag{1}$$

2.2.2. Solvent swelling method

A related alternative method that could yield information on the extent of crosslinking in significantly less time is the evaluation of the solvent swelling properties of the polymer. The analytical basis of this approach is to determine the solvent uptake into the polymer matrix, which is expected to decrease with increased crosslinking [18].

Three specimens (~ 2 g each) were cut from each of the 18 EVA test samples and the exact weight (M_I) was determined on a precision balance. Each specimen was cut into 1 × 1 cm² pieces, put into a sample flask containing ~30 ml toluene (puriss. p.a., SigmaAldrich) and kept there at room temperature (22 ± 1 °C) for 2 h. The solvent was then decanted, liquid solvent adhering to the sample's surface removed by short contact with filter paper, and the weight of the swollen polymer (M_{II}) determined immediately. The measurand is thus the relative weight gain due to incorporation of solvent molecules into the polymer matrix

$$\text{weight gain } [\%] = \left(\frac{M_{II}}{M_I} - 1\right)100, \quad M_{II} \ge M_I \tag{2}$$

2.3. Thermal and mechanical methods

In industrial practice, the Soxhlet analysis suffers not only from its long duration and the use of harmful solvents, but also from a non-absolute correlation between the amount of non-cured and hence leachable material and the actual in-use behaviour of the EVA encapsulants. The main reason for this is that the method cannot differentiate between single and multiple crosslinking of polymer chains. However, the number of crosslinks formed between polymer chains in an elastomer effect is known to strongly affect its mechanical properties, like stiffness and dimensional stability. To overcome this potential problem, a number of different thermal and mechanical methods have been suggested.

2.3.1. Differential scanning calorimetry

The fundamental principle of differential scanning calorimetry (DSC) is to determine the heat flow in or out of a sample vs. its temperature. DSC thus allows measuring thermal transitions of polymers, including glass transition, melting or crystallisation as well as following exothermic or endothermic reactions, including oxidative degradation and/or crosslinking reactions [19].

The DSC measurements were carried out using a DSC 821e instrument (Mettler Toledo GmbH) operated in a double-run mode. A circular specimen disc was punched from the EVA sample, put in a 40 μl pan and closed with a perforated lid. In the first DSC run, the sample was heated up from 25 °C to 200 °C at a constant heating rate of 10 °C/min, held at 200 °C for 10 min and then cooled down to 25 °C at a cooling rate of 10 °C/min. This procedure was repeated in a second run in order to check for any further exothermic energy flow and provide the reference for the subsequent evaluation of the reaction enthalpy.

Two different analytical approaches were conducted in this study. First, the melting points and melting enthalpies were evaluated according to ISO 11357-3 [20]. The "degree of crystallinity" was determined as the ratio of the melting enthalpy of the sample and the melting enthalpy of the (virtual) 100% crystalline polymer; lacking data for EVA, and since the crystallinity of the EVA copolymer is a function of the ethylene content only, the enthalpy of polyethylene (293 J/g) was taken from the ATHAS database [21] and used to calculate the degree of crystallinity [22]. In a second approach, the DSC data was used to detect the remaining crosslinking capability in the various samples and infer the degree of crosslinking by comparing it to the overall crosslinking capability of an uncured EVA foil [10,12,23]. This "DSC degree of crosslinking" (X) was thus determined from the reaction enthalpy $\Delta H_{(Sx)}$ of the crosslinking reaction of the respective test sample in comparison to the reaction enthalpy $\Delta H_{(S0)}$ of the uncured EVA reference (average of all *S*0 samples) according to

$$X_{(Sx)} = \frac{\Delta H_{(S0)} - \Delta H_{(Sx)}}{\Delta H_{(S0)}} \tag{3}$$

2.3.2. Tensile testing

Tensile testing aims at directly measuring key mechanical properties of the EVA samples. The experiments were carried out according to EN ISO 527-3 [24] on a screw-driven Zwick Z010 Allround-Line tensile testing machine (Zwick GmbH) at 23 °C and a test speed of 50 mm/min. Rectangular specimens of 100 mm length and 15 mm width were prepared using a roll-cutter. From a total of at least five specimens per EVA sample, average numbers for the elastic modulus (E), the stress at break (ε_B) and the strain at break (σ_B) were derived.

2.3.3. Shore D0 hardness testing

A potential alternative method to characterize EVA foils could be to measure the hardness of the foil, alternatively that of the laminate, and relate that value to the degree of crosslinking. The approach tested here was based on a standard Shore D0 hardness test for rubbers, which uses a force-loaded indenter with a ball-shaped head to make an indention into a surface and measure the penetration depth [25]. Under the assumption of a dependence of the degree of crosslinking on the mechanical properties of the foil, the measured hardness should reflect this influence.

The experiments were conducted at room temperature (21 ± 1 °C) on a digi test II instrument (Bareiss Prüfgerätebau GmbH) equipped with a ball-shaped head, at a constant load of 44.5 N. Taking into account the viscoelastic behaviour of EVA, the penetration depth reading was taken 50 s after applying the load.

2.3.4. Dynamic mechanical analysis

Contrary to some of the previous methods, dynamic mechanical analysis (DMA) aims at directly measuring the thermo-mechanical properties of the EVA materials, rather than isolated thermal or mechanical properties of uncertain correlation to the overall behaviour. The key motivations behind this are (i) that the mechanical behaviour of EVA depends on both the temperature and the rate of loading, and (ii) that polymers in general, and elastomers in particular, are viscoelastic. Applying a sinusoidal mechanical stress to the sample, the resulting strain and the phase shift can be measured, optionally as a function of temperature. From these values both the elastic part, expressed by the storage modulus E' (G' in shear mode), and the viscous part, expressed by the loss modulus E'' (respectively G''), of the viscoelastic behaviour can be determined [12]. In particular when using the temperature-control option, DMA operated in shear mode has proven to be a suitable tool for measuring the degree of crosslinking of polymers [12], exploiting the fact that the crosslinking reaction directly affects the thermo-mechanical properties of the elastomer.

The experiments were conducted on a DMA 8000 instrument (Perkin Elmer Inc.) in shear mode. Circular samples (9 mm diameter) were prepared and measured at a sample displacement of 20 μm and a test frequency of 1 Hz. The sample temperature was varied from 25 °C to 200 °C at a heating rate of 3 °C/min. Storage and loss modulus G' and G'' and the loss angle δ were calculated from the shear strain and phase shift data and used in the subsequent evaluation.

2.4. Spectroscopic methods

With the motivation of finding potential analytical tools for non-destructive in-line use, another line of investigations comprised the evaluation of various spectroscopic methods. Previous work has indicated that light attenuation in the visible region of the spectrum correlates to the degree of crosslinking [15]. Other investigations have proven that vibrational spectroscopic methods, in particular (mid-)IR absorption and Raman spectroscopy, can be used for monitoring aging and degradation of EVA materials [26–28]; however, no data has been published so far describing the possibility of using such methods for measuring the degree of crosslinking of EVA materials.

2.4.1. UV/vis spectroscopy

The UV/Vis measurements were conducted in classical directed transmission on a Cary 50 UV/Vis spectrometer (Varian Inc.). Three specimens were cut from different areas of each of the 18 different EVA samples, and each specimen measured twice. The absorbance spectra were acquired in dual channel mode for the spectral range 200–1100 nm at 1 nm resolution and an averaging time of 0.1 s. The spectra were subjected to both manual spectroscopic and computer-supported chemometric analysis (principal component analysis and regression; Unscrambler X, version 10.2; Camo Software AS).

2.4.2. Vibrational spectroscopy

Measuring vibrational spectra, i.e. by (mid-)infrared and Raman spectroscopy, is a common and well-established method for a direct and absolute determination of the degree of crosslinking in various polymeric materials. The principle exploited there is to detect the amount of reactive groups, e.g. unsaturated bonds or isocyanate groups, before, during and after the crosslinking reaction by their characteristic spectral features, giving a direct quantitative value for the extent of crosslinking. In the case of EVA materials used in PV modules, however, the situation is significantly different, since these EVA materials contain no dedicated crosslinking groups. Instead, the radical crosslinking reaction, which is supposed to proceed primarily via the vinyl acetate side chains, transforms terminal methyl ($-CH_3$) groups into methylene ($-CH_2-$) groups. The only spectroscopically detectable change would thus be a change of the relative intensities of the characteristic CH_x features. Since the extent of crosslinking in the cured state of EVA is low, these changes in the CH-region of the vibrational spectra are expected to be weak, but might still be significant. The experimental validation of this assumption was conducted in parallel using two complementary vibrational spectroscopic techniques: *mid-IR absorption spectroscopy* and *Raman spectroscopy*.

Mid-IR spectroscopy: Mid-IR spectra were acquired using a Nicolet Nexus 870 (Thermo Electron Corp.) equipped with a liquid nitrogen-cooled MCT detector, (i) in transmission and (ii) in attenuated total reflection (ATR) using a Smart DuraSamplIR 9 reflection HATR accessory. Three specimens were cut from different parts of each of the 18 different EVA samples, and each specimen measured twice. The spectra were recorded in absorbance mode, co-adding 100 scans over the range 4000–650 cm^{-1} (2.5–15.4 μm) at 4 cm^{-1} spectral resolution. For the ATR measurements, the samples were pressed against the diamond ATR crystal with a force of 2 N. The recorded absorbance spectra and their first and second derivatives were first evaluated manually, including a quantitative evaluation of band areas of relevant spectral features. In addition, computer-supported chemometrics tools (Unscrambler X, version 10.2; Camo Software AS) were deployed.

Raman spectroscopy: The Raman spectra of the EVA samples were recorded using a confocal LabRam 800 h Raman system (Horiba Jobin Yvon) equipped with a computer-controlled motorized XYZ stage, a 633 nm excitation laser, and a Peltier-cooled 1 in. CCD camera with 1024×256 pixels as detection system. An Olympus LUCPlanFL N objective with cover slide correction with 40-fold magnification and NA 0.6 was used. The pinhole was closed to 300 μm, the spectral slit set to 100 μm and the integration time per spectrum was 20 s. The spectra were recorded in the spectral region 100–3500 cm^{-1} with a spectral resolution of $\sim$2 cm^{-1} (300 lines/mm grating). The signal was averaged over a measuring area of 30×30 μm² using the DUOSCAN™ system. Four spectra were recorded for each sample at different positions, yielding a total of 72 spectra. The acquired spectral data sets were subjected to chemometric analyses using the software suite OPUS (OPUS 7.0, Bruker Optics) with the extension OPUS QUANT. A multivariate calibration was performed for the CH stretching vibration region (3050–2780 cm^{-1}), assuming the *S*0 samples to be 0% crosslinked and the S10 samples to be 100% crosslinked, and then using all 72 spectra for cross-validation.

2.5. Acoustic methods

The group of acoustic techniques is methodologically related to the mechanical analysis methods, but is inherently non-destructive and could thus eventually be used for in-situ testing

of assembled modules. Two fundamental principles were tested: in the first approach, the changes in the vibration resonance conditions, i.e. the *resonance frequency* and the *resonance vibration amplitude*, of suspended EVA films were detected and correlated to the change of the mechanical properties of the material during crosslinking. As a second approach, the materials' sound propagation/attenuation properties, which are also influenced by a material's stiffness and its degree of crosslinking, were evaluated.

2.5.1. Laser Doppler vibrometry

In a first approach to assay the feasibility of correlating the resonance conditions of a suspended EVA membrane with the degree of crosslinking, a recently developed setup [29] comprising a laser Doppler vibrometer as detector and a frequency-variable acoustic actuator (speaker) was used. The setup comprises a coaxial vertical arrangement of the respective EVA sample clamped between two aluminium plates with circular 25 mm apertures, a speaker (W 100S—4 Ω, Visaton GmbH) mounted below the sample and an MSA500 laser Doppler vibrometer (Polytec Inc.) above the specimen. For the measurement, the speaker performed a 20–500 Hz frequency chirp at 0.156 Hz resolution, and the ensuing vibrations of the test sample were picked up by the vibrometer. Plotting the amplitude of this oscillation against the actuation frequency allowed the determination of the resonance frequency and the corresponding oscillation amplitude, both of which were used in the subsequent evaluation.

2.5.2. Laser scanning vibrometry

In a related approach aiming at measuring the EVA status in-situ in the process, the effect of differently crosslinked EVA encapsulants on the resonance conditions of entire PV modules (here represented by 34×34 cm² mini-modules without PV cell) were assayed using laser scanning vibrometry. In this setup, the test module was supported on two opposing edges and acoustically excited by a speaker emitting a 1 Hz–10 kHz white noise signal toward the glass frontside. The resulting vibrations were picked up from the module backside using a PSV 300 scanning vibrometer (Polytec Inc.). The frequency modes were then calculated from this data using a Fourier analysis.

2.5.3. Scanning acoustic microscopy

Scanning acoustic microscopy (SAM) is a non-destructive acoustic method commonly used for detection and visualisation of imperfections, voids and defects in multilayer structures, like assembled PV modules. The signal generating principle is based on a scanning pixel-wise measurement of acoustic impedance (i.e. acoustic density), which is then converted into a corresponding grey-scale pixel value. The working hypothesis was that the crosslinking of the encapsulant should influence the sound propagation properties in the material as well as its adhesion to the co-laminated elements.

For the experimental validation, an SAM 400 device (PVA TePla Analytical Systems GmbH) used in pulse-echo mode was deployed. The test samples used were laminated onto a polyamide backsheet to enable studying possible interfacial effects. Water was used as ultrasonic wave transmitter, with the excitation frequency set to 75 MHz, yielding a best possible spatial resolution of 20 μm.

3. Results

3.1. Chemical methods

The results obtained from the Soxhlet analysis show a gel content/lamination time relationship (Fig. 1, left) that is typical for rapidly curing EVA materials: strong time dependence at the beginning, followed by an inflection towards stable values after ~3–4 min. In the present case, the used EVA composition exhibited gel contents > 80% for lamination times > 4 min, with a predicted maximum gel content of 90 ± 1%. The deviation from the theoretical maximum of 100% could be explained to some extent by the leaching of non-polymer additives (i.e. UV and other stabilisers, crosslinker, etc.), partly by a non-crosslinking of some of the polymer. What can also be seen is a significant decrease in variability with increasing lamination times: samples with 2 min and – to a lesser extent – 4 min lamination time show a high variability, indicating an inhomogeneity in the crosslinking at early states of the reaction that levels off as the reaction approaches completion.

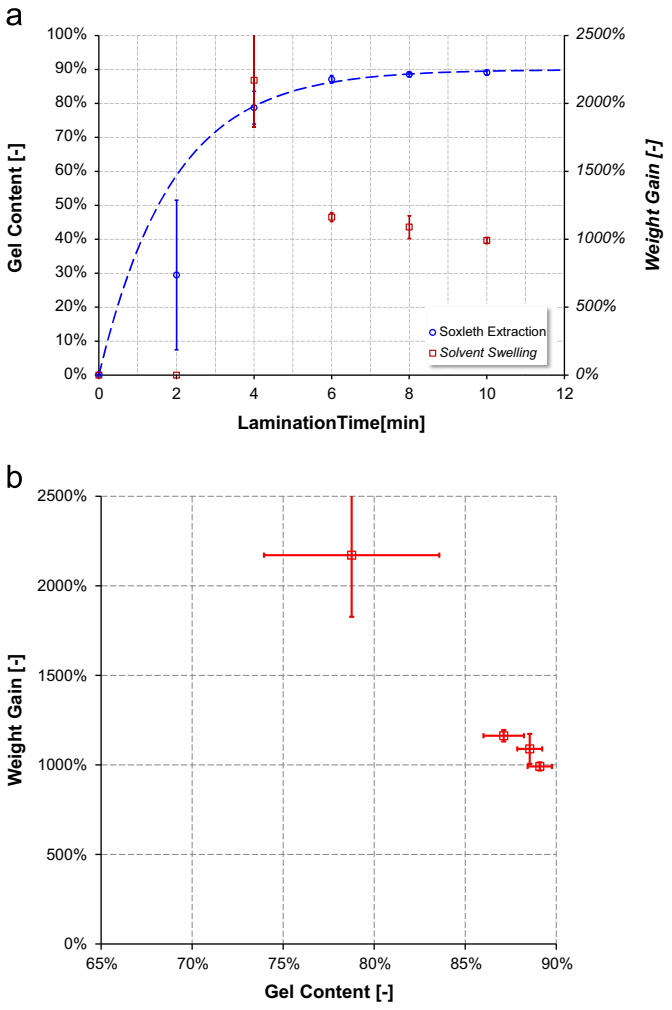

Fig. 1. Left: dependence of the EVA gel content according to the Soxhlet extraction method and of the weight gain according to the solvent swelling method; right: correlation between the two methods.

The swelling method yielded comparable results (Fig. 1, left), with the main difference that it proved impossible to get meaningful results for samples *S0* and *S2*. The reason for this is the complete (*S0*) respectively partial (*S2*) dissolution of the polymer in the solvent, which prevented measuring *S0* samples and rendered the results for *S2* samples meaningless. A correlation analysis between the two methods (Fig. 1, right) indicates a correlation between the methods that could be used practically, if validated in a further study. While the Soxhlet method is definitely preferable for lowly crosslinked materials, i.e. short lamination times, the solvent swelling approach could be an interesting, since much faster, method for monitoring the later stages of the crosslinking reaction, i.e. of EVA materials where curing is approaching completion.

3.2. Thermal and mechanical methods

3.2.1. Differential scanning calorimetry

Fig. 2 shows typical DSC thermograms of an uncured *S*0 and an almost fully cured *S*10 EVA sample. Common to all investigated specimens is a melting range between 30 and 70 °C, visible as a negative peak in the thermogram. This temperature range comprises a peak maximum at ~45 °C relating to secondary crystallisation [21,30,31], and a shoulder at ~60 °C, which is attributed to the thermo-dynamic melting point of EVA. From this feature, a crystallinity of approximately 9% for the uncured EVA and of around 7% for the most strongly crosslinked EVA samples *S*8 and *S*10 could be derived. While this trend corresponds to the theory predicting a reduction in polymer crystallinity with increased crosslinking, the effect on the crystallinity of PV-grade EVA is too weak in comparison to in-material variations to be usable as a reliable measurand for the degree of crosslinking.

The second relevant feature is the exothermal, and hence positive, reaction peak of the crosslinking reaction, which occurs in the range 120–190 °C. This peak, which relates to the reaction heat generated in the radical crosslinking reaction, varies strongly with the (residual) amount of crosslinker in the EVA samples. Fig. 3 (left) shows a relationship between the DSC Degree of Crosslinking and the lamination time that is in good agreement with a first order reaction kinetically limited by the thermal homolysis of the crosslinker. The reaction is nearly completed after ~7 min, visible in a sloping-off of the curve. Furthermore, fitting reaction kinetics to the experimentally determined data set predicts a maximum average DSC degree of crosslinking of $84 \pm 4\%$ (dashed curve in Fig. 3, left). This indicates either an activation of only ~85% of the crosslinker at the standard lamination temperature of 150 °C, or an interference by another thermally induced reaction in the polymer.

The comparison of the DSC degree of crosslinking to the gel content as determined by the standard method showed some significant deviations (Fig. 3, right), with the Soxhlet method yielding higher values. This is not unexpected, since the two measured quantities differ in their physico-chemical principles: the Soxhlet extraction method determines the amount of crosslinked and hence insoluble polymer chains, while the DSC measures the amount of crosslinker remaining in the polymer after lamination and estimates the amount of consumed crosslinker from that. Furthermore, any correlation of this type would be strongly influenced by the chemical nature and the initial amount of crosslinker in the material.

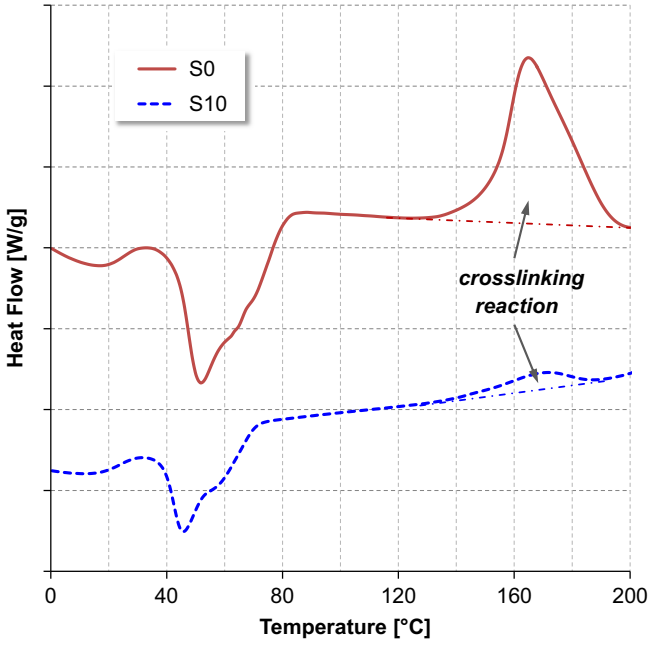

Fig. 2. Typical DSC thermograms of uncured (sample *S0*) and partially cured (sample *S10*) EVA (stacked plot).

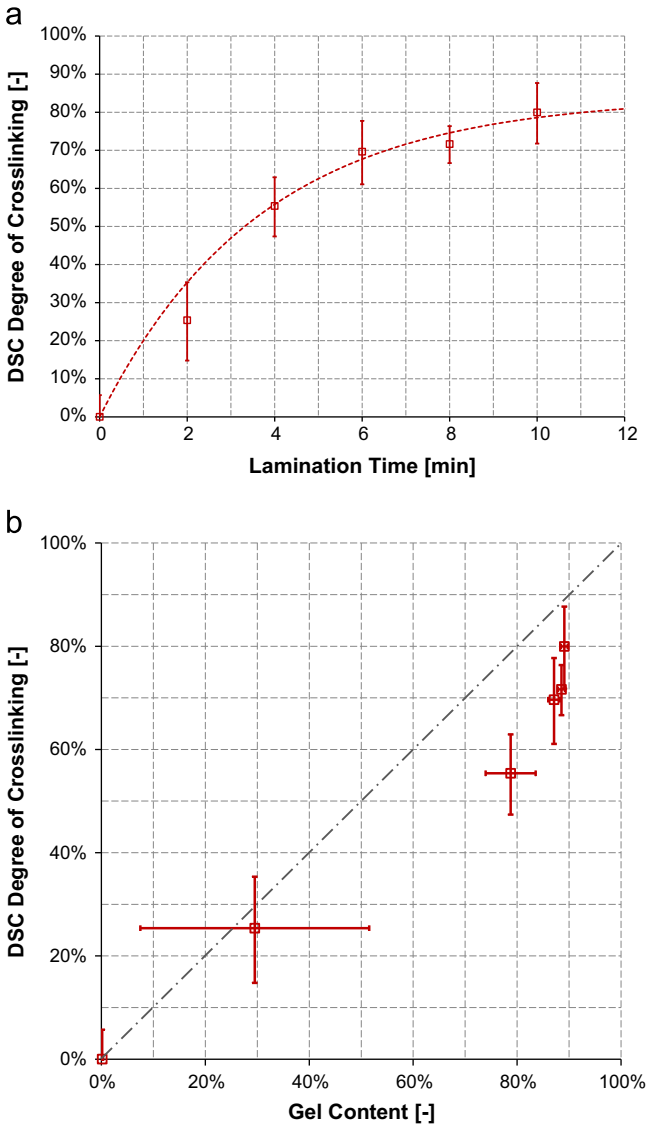

Fig. 3. Degree of crosslinking obtained by DSC vs. lamination time, overlaid with its first order reaction kinetics fit (dashed line) (left), and vs. the gel content according to the Soxhlet reference method (right).

Besides inevitable variations in concentration between batches, this relates to another omnipresent problem of many curable EVA materials: a notoriously inhomogeneous distribution of the additives in the encapsulation foils. To avoid a premature crosslinking during film processing, the curing agent has to be dispersed at relatively low temperatures, making it difficult to guarantee a uniform and fully homogenous distribution of the curing agent in the extruded film [32].

3.2.2. Tensile testing

The investigation into the influence of the degree of crosslinking on the mechanical properties of EVA yielded mixed results. While no significant influence on the elastic behaviour was observed, the effect on the post-yield plastic deformation

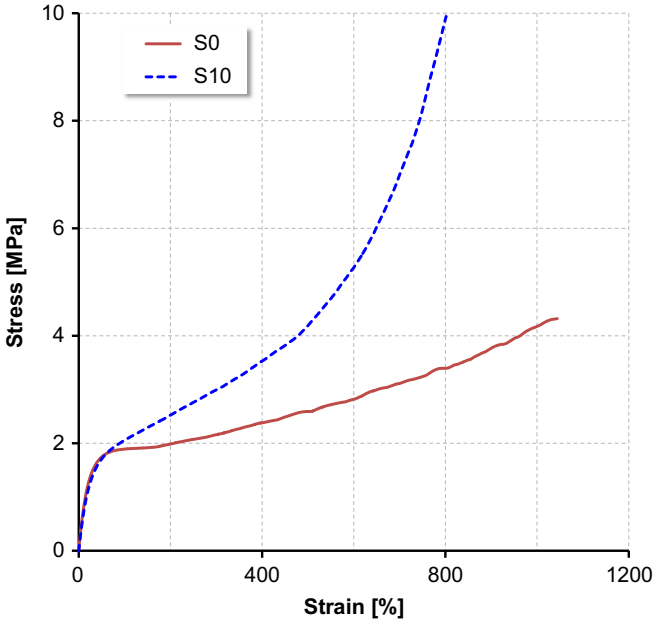

Fig. 4. Characteristic stress–strain curves of uncured (*S0*) and fully cured (*S10*) EVA samples.

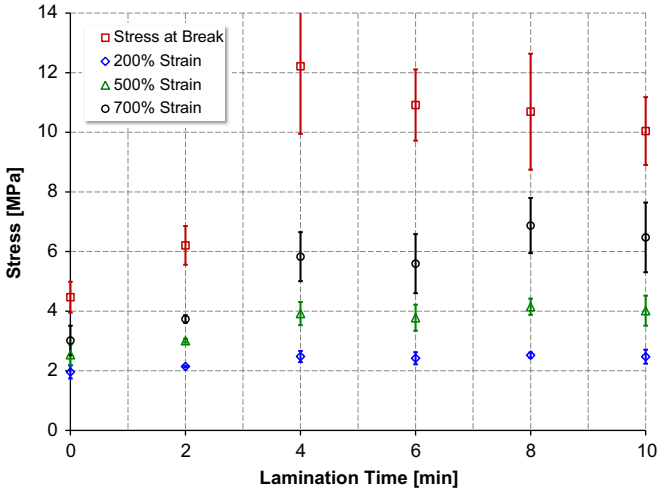

Fig. 5. Tensile test results of EVA films vs. lamination time.

properties is pronounced. Fig. 4 shows representative stress–strain curves of uncured (i.e. *S*0) and fully cured (i.e. *S*10) EVA films illustrating the general stress–strain behaviour of the EVA materials. Basically, and in agreement with requirement profile for elastomeric encapsulants, all materials show a highly ductile behaviour, high flexibility and no pronounced yield point.

Evaluation of the elastic modulus, i.e. the slope to the stress/strain-curve in the elastic deformation region at low strains, yielded identical values of 9–10 MPa for all samples, without significant dependence or even a discernible trend vs. the state of crosslinking. This agrees with the general room-temperature behaviour of most weakly crosslinked elastomeric materials, where the contribution of the few extra covalent bonds connecting the polymer chains is negligible in comparison to the polymer matrix and the intermolecular forces therein. In contrast, significant changes could be observed in the post-yield region. While all samples exhibited an essentially bi-linear stress/strain relationship, the cured samples are significantly stiffer in this region and the strain-at-break values are lower. This can be attributed to the three-dimensional widely meshed polymer network, which restricts re-orientation and slipping of the polymer chains, thus significantly constraining the plastic deformation.

Evaluating the stress-at-break showed significance only for partially crosslinked materials, i.e. short lamination times, and is subject to substantial variability (Fig. 5). Measuring the stress required to achieve a pre-set strain proved a better alternative, though the analytical sensitivity and reliability depends very much on set strain level: at low strains poor sensitivity is observed, while higher levels come with increased variances (Fig. 5). The same applies when correlating the stress-at-strain values to the gel content derived from the Soxhlet experiments (Fig. 6, left) and the DSC Degree of Crosslinking (right).

Altogether, while the trends prove potentially exploitable dependencies of stress-at-strain measurands on the curing state, the presently inherent variability of the measurement procedure proved too strong for setting up a reliable calibration to infer the crosslinking state from tensile tests. The source of this problem has not been fully investigated. Determining the thicknesses of the samples gave values of 460 ± 15 μm for all specimens, without statistically relevant relation to the curing. While this contributes to the value scattering, it cannot fully explain it; assumedly, other relevant factors include the inherent variability of the tested specimens, minor deviations in specimen preparation, and problems related to reproducibly clamping soft materials.

3.2.3. *Shore D0 hardness testing*

While the Shore D0 method showed a tentative dependency on the lamination time of the EVA encapsulant material in this blinded study, this effect is firstly limited to short lamination times/ low degrees of crosslinking and secondly overlaid by a strong variability of the measured hardness data (Fig. 7), effectively rendering these results useless for calibration purposes. A reason for this may be the low thickness of the EVA samples; standard Shore D0 testing of elastomers usually uses mm-thick specimens.

Another key disadvantage observed in related experiments measuring PV laminates is mechanical damaging of the solar cells by the test pin load [14]. For a possible further investigation it would be necessary to set the prescribed standard conditions aside and use e.g. an adapted indenter with larger contact area, or apply less force.

3.2.4. *Dynamic mechanical analysis*

When evaluating the obtained DMA results, the influence of the lamination time on the temperature dependencies of the shear modulus and the damping factor is obvious (Fig. 8). While for the cured *S10* samples the *shear modulus G′* shows an initial sloping down that settles to a constant value at around 70 °C, the non-cured *S0* samples show a strong drop in the range 60–75 °C, i.e. the melting range of EVA (Fig. 8, left). The modulus then slopes further downward until it rapidly turns upward at ~125 °C. This confirms the DSC results, which indicate the radical crosslinking reaction to be fully activated at 120–125 °C. The increase in storage modulus can thus be attributed to the activation of the crosslinking and the subsequent formation of a three-dimensional polymer network. At around 170 °C, the storage modulus levels off and reaches the values of the fully crosslinked material. Both observations agree with a completion of the crosslinking reaction. The *damping factor* $\tan\delta$ exhibited a mirror image behaviour (Fig. 8, right): the melting region starting at ~60 °C is accompanied by a strong increase of the damping factor, which can be attributed to the high mobility of the polymer chains in the molten state. The damping factor peaked at ~125 °C, at which temperature the crosslinking fully sets in and subsequently reduces the mobility of the polymer chains due to the increasing crosslinking density.

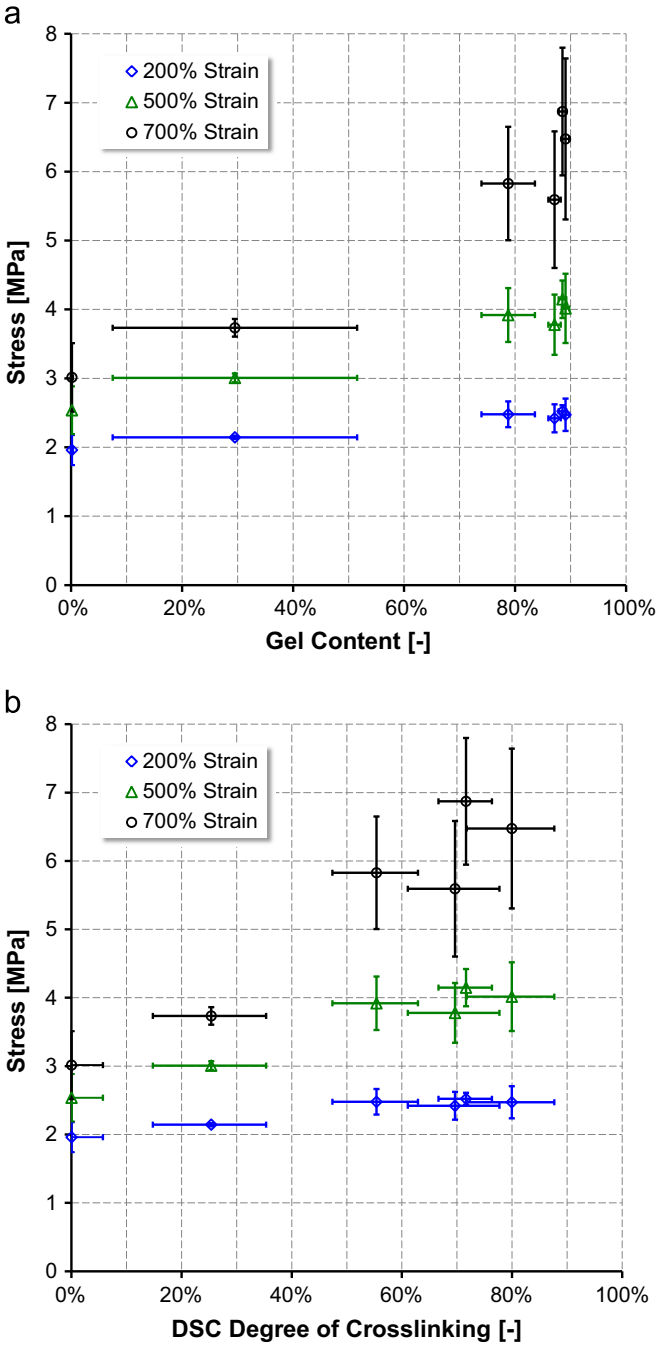

Fig. 6. Stress levels required to achieve specific strain states vs. gel content (left) and vs. the DSC Degree of Crosslinking (right).

In the melting region, both the shear modulus G' and the maximum damping factor $\tan\delta_{max}$ are strongly influenced by the crosslinking state of the elastomer. While the traditional factor to be correlated is the minimum of the storage modulus of the temperature curve, this value can be influenced by various external factors, like the positioning and clamping of the samples, the contact between the shear plates and the specimen, and by the uniformity of the specimen preparation [18]. To eliminate these variables, a recently developed self-referencing alternative method for determining the degree of crosslinking from DMA data was applied here. This method derives the slopes of the linear sections to either side of the shear modulus minimum, and of the steady post-crosslinking section, as illustrated in Fig. 8 (left). The intersections of these linear

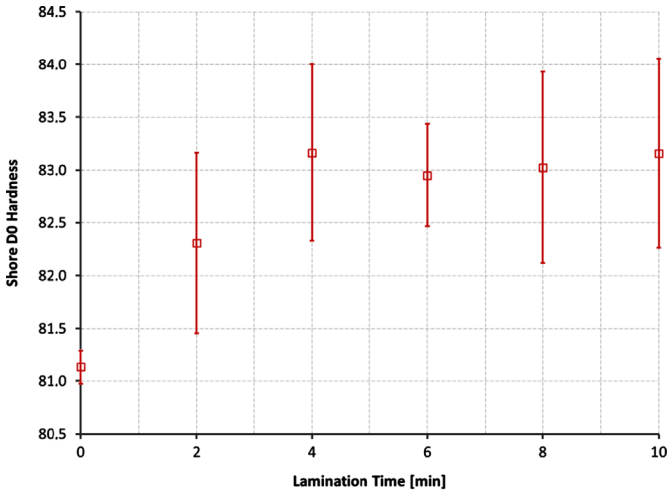

Fig. 7. Shore D0 hardness values vs. lamination time.

extrapolations to either side of the minimum yield the measurement point G'_1, while the intersection of the rising slope and the steady section give the reference modulus G'_2. Taking the G'_2/G'_1 ratio as measurand yields highly reliable values with minimised measurement variability; a further advantage of the method is that the measurand always converges asymptotically to 1 for fully cured materials. As an alternative approach, the maximum of the damping factor was evaluated, which also yields reliable and reproducible analytical readings.

Evaluated against the lamination time, both parameters showed similar relationships (Fig. 9): the values decrease strongly over the early phase of crosslinking, but show little to no effects at higher times. Investigated in detail, the modulus ratio approach showed a good sensitivity for following the EVA crosslinking in its early stages, i.e. up to 4 min lamination time ($\sim$ 78% gel content), but could not reliably differentiate between samples with longer crosslinking times. Measuring the maximum damping factor yielded a similar decrease with an inflection point at 5–6 min, corresponding to $>$ 80% gel content, followed by a weak but distinct further time dependency. Fundamentally similar relationships with varying degrees of non-linearity were also found when conducting correlation analyses to the standard reference measures used in PV characterisation, i.e. the gel content (Fig. 10, left) and the degree of crosslinking determined from DSC measurements (Fig. 10, right). In either case, the analytical reliability of the DMA measurements was found to be superior to those of the reference methods.

3.3. Spectroscopic methods

3.3.1. UV/vis spectroscopy

With exception of the *S0* specimens, the vis-range absorption spectra showed a steady directed transmission of $>$ 90% for wavelengths $>$ 600 nm; for the range 400–600 nm, the absorptions increase slightly (Fig. 11, left). The *S0* spectra showed a similar spectral behaviour, but with a 1.0 AU offset i.e. only $\sim$ 10% directed transmissibility. In the UV region below 400 nm, the absorptions increase rapidly due to the presence of UV stabilisers.

Conducting a detailed spectral analysis using a principal component analysis (PCA) yielded a clear separation of the *S0* samples from the others along the first principal component axis, and a good separation of the samples *S2*–*S10* on the second (Fig. 11, right). The latter could be assigned to subtle changes in the range 360–600 nm. This spectral range and the observed changes in the spectrum indicate a change in the scattering behaviour of the polymer as the root cause; pending further

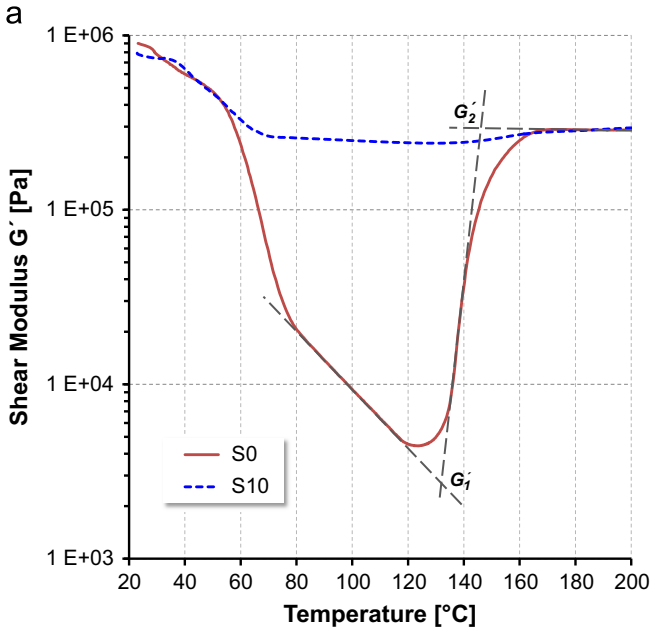

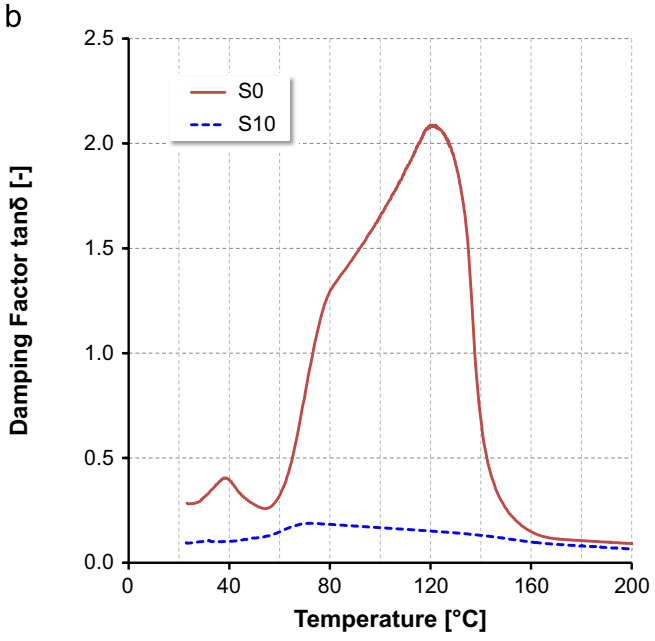

Fig. 8. Typical shear modulus – temperature (left) and damping factor – temperature (right) of uncured and cured EVA films.

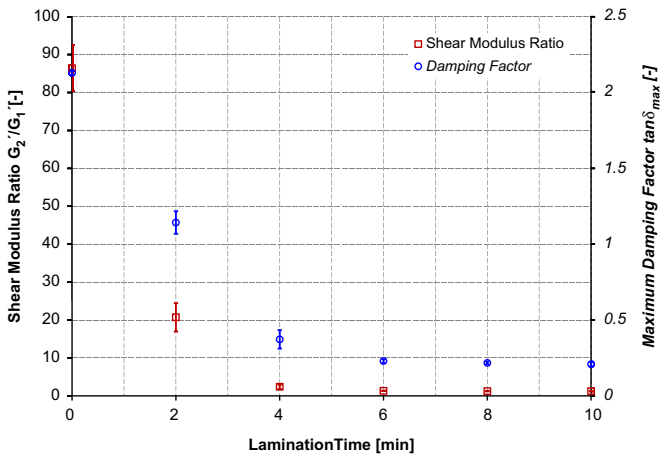

Fig. 9. Shear modulus ratio (left axis) and maximum damping factor (right axis) obtained from shear-mode DMA measurements vs. EVA lamination time.

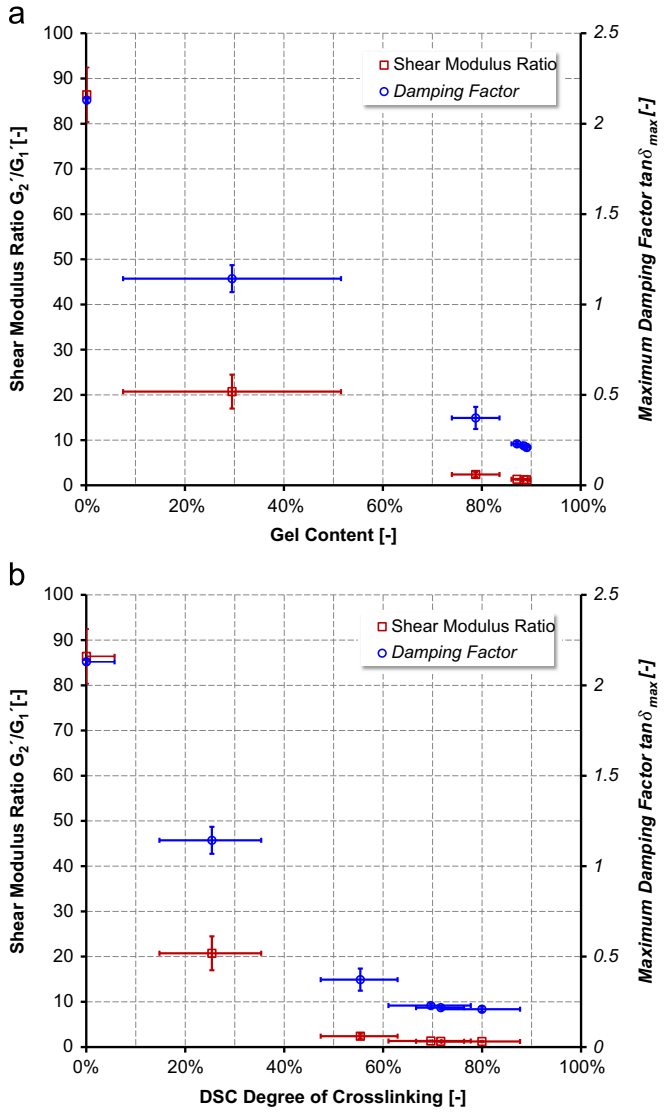

Fig. 10. Shear modulus ratio (left axes) and maximum damping factor (right axes) obtained from shear-mode DMA measurements vs. the gel content obtained from the Soxhlet method (left) and vs. the DSC degree of crosslinking (right).

investigations, one possible explanation is a change in polymer crystallinity with crosslinking. Attempting a quantitative correlation using a principal component regression (PCR) analysis yielded a fundamentally good correlation to the curing state, but overlaid with inherent variances of the measured values that render absolute quantification and method calibration problematic. This agrees with the findings of the first DSC approach measuring the degree of crystallinity: the crystallinity of the polymer changes with crosslinking, but the effect is weak and hence easily obscured by chance interferences.

3.3.2. *Mid-IR spectroscopy*

As expected, the spectral features of the base material EVA dominate the mid-infrared spectra (Fig. 12), comprising different

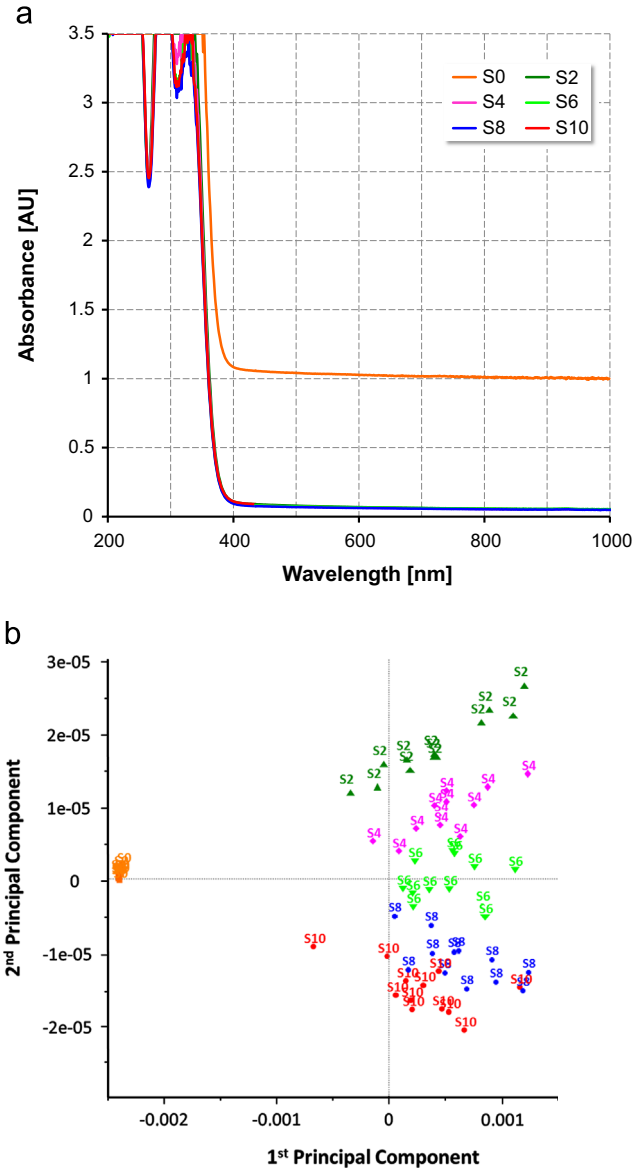

Fig. 11. Typical UV/vis absorption spectra (left) and Principal Component Analysis results of the EVA sample's UV/vis absorption spectra for the spectral range 360–960 nm (right).

aliphatic CH_x vibrations (3000–2800 cm^{-1}, 1500–1400 cm^{-1} and 1000–700 cm^{-1}) and the characteristic bands of the vinyl acetate component (1733, 1365 and 1234 cm^{-1}).

When measuring the ~460 μm thick EVA specimens in standard transmission mode, the incident IR radiation is fully absorbed at the wavelengths of the main polymer absorption bands (Fig. 12, upper spectra; cut-off at 3.5 AU, i.e. 0.03% transmission); the spectral features of the polymer itself could hence not be evaluated. The remaining spectral features showed no relation to the lamination time, with exception of two sharp peaks at 1772 and 1646 cm^{-1} that decrease with increasing lamination times. These bands could be assigned to peroxycarboxylic acids, i.e. the crosslinking agent itself; consequently, the bands are present in the *S*0 samples but no longer detectable against the background in the cured *S*10 specimens.

Evaluating the peak areas of these two specific features against the lamination time yields a clear relationship (Fig. 13, left) that can be perfectly fitted with a corresponding first-order reaction curve characteristic for homolytic reactions (when eliminating the notoriously outlying *S*2 data). In addition, a correlation analysis against the standard methods showed a practically linear relation to the Soxhlet-derived gel content (Fig. 13, right). Extending that analysis by comparing the first-order temporal dynamics to those of the Soxhlet gel content method (Fig. 1, left) and the Raman approach (Fig. 15) showed excellent agreement. Yet, a comparison of the time dependency in Fig. 13 to that of the DSC Degree of Crosslinking (Fig. 3, left) shows significantly slower dynamics there. This is somewhat surprising since these two methods measure the same analyte, i.e. the residual amount of crosslinker present in the sample after lamination, and would merit further investigation into.

One practical disadvantage of this method is that it is an indicative method detecting the residual amount of crosslinker, rather than the actual crosslinking itself. The method thus has to rely on a constant initial crosslinker concentration, or would require regular analysis of the incoming EVA material. As an alternative, it was attempted to correlate the CH_x absorption features of the base material itself to the progress of curing by recording ATR spectra of the EVA samples. As a surface-sensitive technique, ATR has an information depth of typically just a few μm, thus averting the complete absorption of the radiation at the relevant peaks (Fig. 12, lower spectra) and enabling their evaluation.

The following in-depth analysis indeed showed changes of the CH_x absorptions with the duration of the lamination, affecting in particular the relative intensities of the CH_2/CH_3 valence vibration

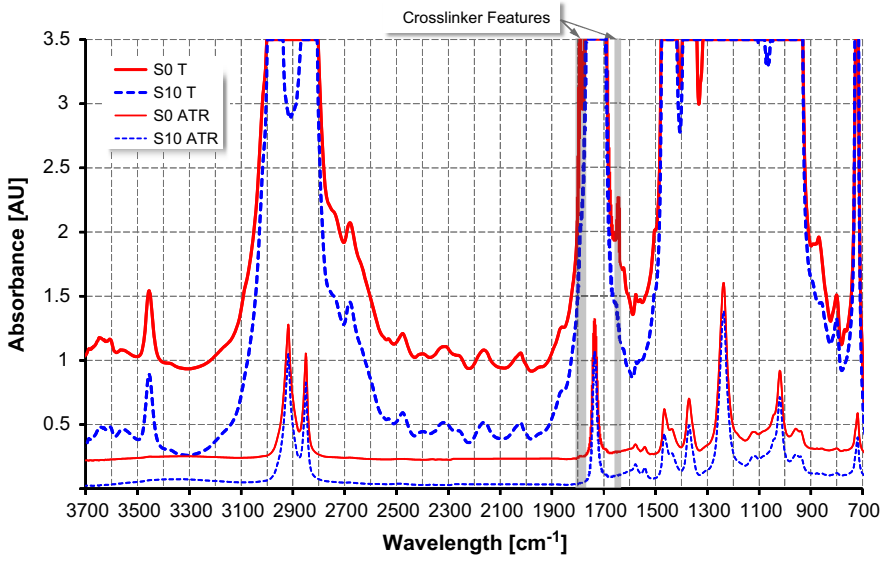

Fig. 12. Typical mid-IR absorption spectra of an uncured (*S0*) and a completely cured (*S10*) EVA foil, measured in transmission (*S0 T*, *S10 T*) and using an ATR probe (*S0 ATR*, *S10 ATR*) (stacked plot).

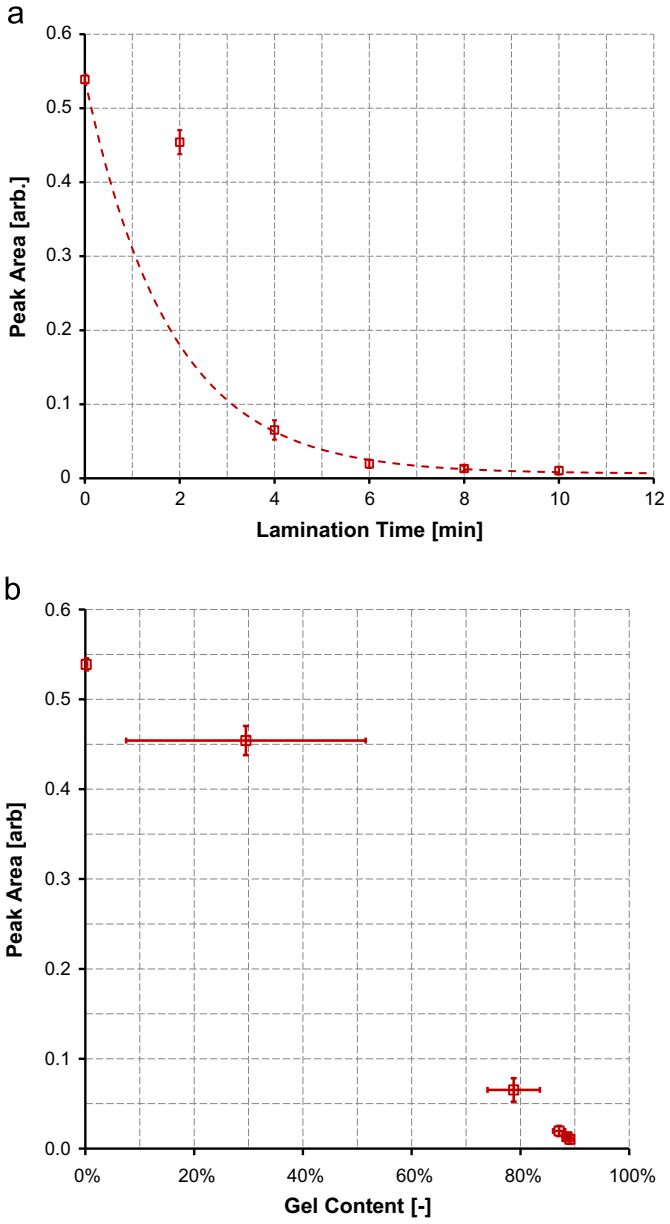

Fig. 13. Peak area of the crosslinker absorption band vs. lamination time, overlaid with its first order reaction kinetics fit (dashed line) (left), and vs. the gel content according to the Soxhlet extraction reference method (right).

duplet at 2918 and 2850 cm^{-1} and in the so-called fingerprint region at 960–930 cm^{-1}. This would support the established crosslinking model, i.e. the transformation of terminal methyl groups into methylene bridges between the polymer chains. However, despite a reproducible trend, attempts to establish a quantitative model to predict the degree of crosslinking from mid-infrared ATR spectra failed to meet the established analytical quality criteria. Main reasons for this are (i) the low amount of created crosslinks in comparison to the overall amount of methyl and methylene groups in the polymer, and (ii) an inherent variability of the material.

3.3.3. Raman spectroscopy

At first glance, the Raman spectra of differently crosslinked EVA samples (Fig. 14) show hardly any difference from the spectroscopic point of view. However, detailed spectroscopic and chemometric analyses revealed subtle spectral changes in the CH–stretching vibration region, i.e. 3000–2800 cm^{-1}. With increasing crosslinking, the intensity of the spectral features of the methylene groups (–CH–) increase relatively to the intensity of the spectral peak attributed to the CH_3– stretching vibration (Fig. 14, inset). This agrees well with the assumption that the crosslinking is proceeding primarily via a radical reaction of the vinyl acetate's terminal methyl groups (–CH_3), transforming them into methylene bridges.

With only around 1% of the terminal CH_3-groups participating in the crosslinking reaction, the observed spectral effect is minor, but still proved significant. Fig. 15 shows the results of the predicted Raman crosslinking values vs. lamination time. With exception of the *S2* samples, which yielded results significantly below the expected curve, the values fit nicely to a pseudo first-order reaction kinetics curve (dashed line in Fig. 15) that stands in agreement to the kinetics established from both the Soxhlet method and the IR detection of the decrease in the amount of crosslinker. Verifying the values predicted by the Raman method against the gel content according to the Soxhlet method (Fig. 16, left) and the degree of crosslinking determined by DSC (Fig. 16, right) yielded approximately linear relationships in good proximity to the expectancy values.

In comparison to the Soxhlet method, the Raman method slightly under-predicts the degree of crosslinking at higher lamination times (Fig. 16, left). This agrees with the theory, since a single bond formed during curing may suffice to make a polymer chain non-leachable and hence contribute to the gel content, while the Raman method measures the amount of actually formed crosslinking bonds. When using the enthalpy-based DSC method as reference, the data obtained from the Raman method tend to over-predict the degree of crosslinking at higher lamination times (Fig. 16, right), a deviation that would merit further investigation into. Another observation is that the *S2* samples yield comparable results with all methods, despite their strong deviation from the expected values in all kinetics curves. This indicates a systematic problem with the *S2* samples; one plausible explanation would be that it takes some time to bring the EVA foil inside the PV laminate stack to full temperature. Thus, the actual crosslinking time, i.e. the period the EVA film is at 150 °C, would be significantly shorter than the contact time with the heating plate, which was taken as measure for the lamination time. This would affect the samples taken after short lamination times more strongly than those sampled after longer ones, and could also explain at least some of the strong scattering of the *S2* samples observed with many of the investigated methods. The effect will have to be further investigated and verified in subsequent studies.

3.4. Acoustic measurements

3.4.1. Laser Doppler vibrometry

The evaluation of the mechanical vibration states of EVA foils established a good correlation between the maximal vibration amplitude and the lamination time, and also some correlation between the resonance frequency of the respective specimen and the lamination time (Fig. 17). While the results are in agreement with DMA measurements showing a decrease in the damping factor with increasing degrees of crosslinking (Fig. 8), thus explaining the increased amplitudes under resonance conditions, the observed close-to-linear relationship to the lamination time is somewhat unexpected and will require further investigation.

3.4.2. Scanning laser vibrometry

Other than with the EVA foils alone, no significant effect of the curing state of the EVA encapsulant on the mechanical vibration properties of an entire assembled PV module could be found. Both

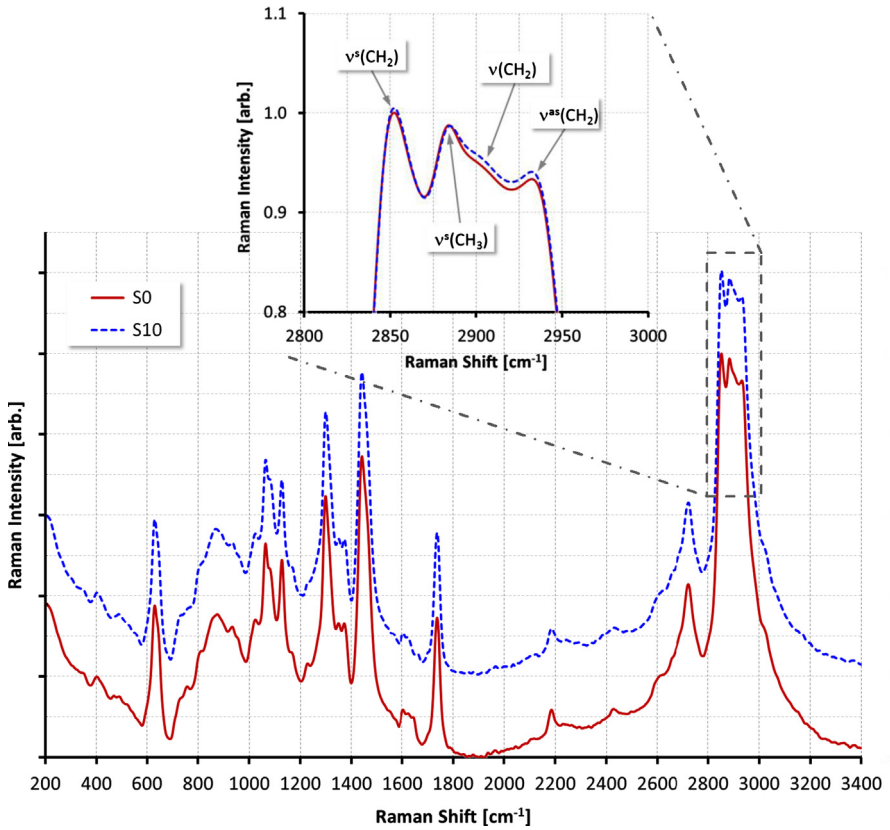

Fig. 14. Typical Raman spectra of an uncured (*S0*) and a completely cured (*S10*) EVA sample (stacked plot); the inset shows a magnification of the CH_2/CH_3 stretching vibration region found most relevant for the discrimination between differently cured EVA specimens.

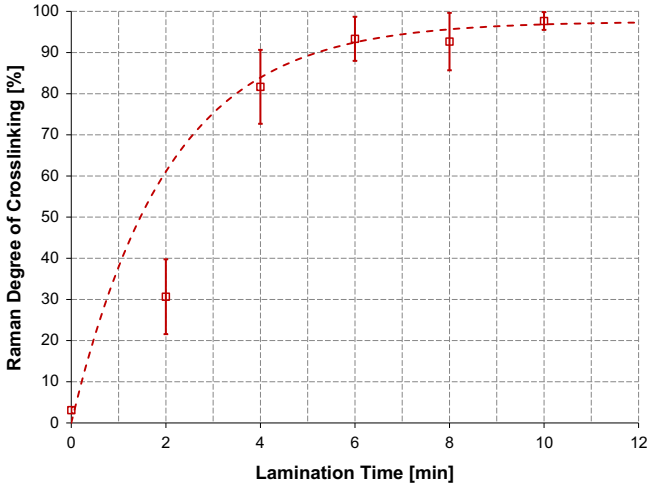

Fig. 15. Degree of crosslinking according to the Raman approach [%] vs. lamination time, overlaid with a pseudo-first order reaction kinetics curve fitted to the data set (dashed curve).

the resonance frequency and the amplitude maximum showed no discernible correlation, and poor repeatability. It would appear that the effect of the encapsulant on the overall mechanical (vibration) properties of the module is negligible in comparison to the contributions by the solar glass and the backsheet.

3.4.3. *Scanning acoustic microscopy*

The EVA samples were analysed by SAM for differences in their surface structure and the propagation times of the acoustic waves through the samples. The subsequent correlation analyses of these measurands vs. lamination time, or any of the other measures of the crosslinking state, yielded no significant correlations. This can be attributed to the generally low acoustic impedance of EVA materials, which is but marginally affected by the low degrees of crosslinking occurring here. Evaluating the SAM images of the sheet surfaces shows the *S0* samples to be clearly different (Fig. 18), showing a surface roughness correlating with the low UV/Vis transmittance measured for the same samples. The samples that had been exposed to a heat treatment all show similarly homogeneous surfaces without relevant features that could be related to the curing conditions.

4. Conclusions

4.1. *General findings*

One main result of this comparative study of 16 different analytical approaches for determining the crosslinking status of EVA encapsulants for PV modules is that a range of different methods could be used for off-line applications; an overview is given in Table 1. Apart from the Soxhlet reference method, seven methods showed a good correlation with the curing status of EVA. Three more techniques exhibited a fair correlation to the amount of crosslinking, but would require further research to qualify them as reliable analytical methods. A remarkable fact in this context is that the physico-chemical basics of these (potential) analytical procedures, and with them the actual analytes, vary widely. Methods showing a good to fair correlation to lamination time and the reference method measure either (i) the formation of the actual crosslinks (IR or Raman spectroscopy), (ii) various parameters describing the elastic respectively visco-elastic properties of the EVA materials (DMA or Laser vibrometry), or (iii) the

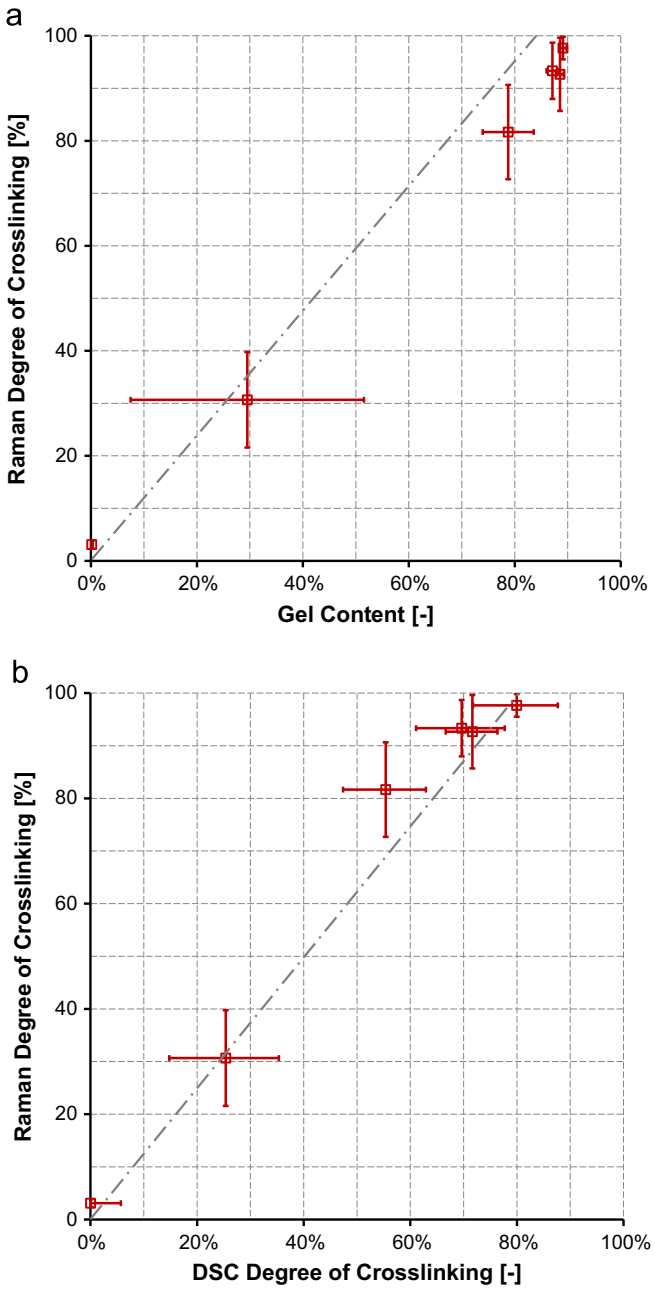

Fig. 16. Degree of crosslinking according to the Raman approach vs. the gel content according to the Soxhlet standard method (left) and vs. the DSC Degree of Crosslinking (right); dash-dotted lines represent the expectancy functions of the applied calibration model.

residual amount of cross linker present in the material after lamination (DSC, IR spectroscopy).

A second interesting fact emerging from this study is that the correlation functions of all these methods are somehow different when investigated in detail. While this is hardly surprising when comparing results obtained with analytical techniques using fundamentally different measuring principles, in several instances even fairly similar methods showed significant differences in the obtained results. One example for this would be the evaluation of the thermo-visco-elastic properties using dynamic mechanical analysis, which yields different correlation functions depending on the chosen measurand (see Figs. 9 and 10). Another illustrative example are the different kinetics of the crosslinker consumption observed with DSC (Fig. 3, left) and mid-IR transmission spectroscopy (Fig. 13, left) for identical samples. At the same time,

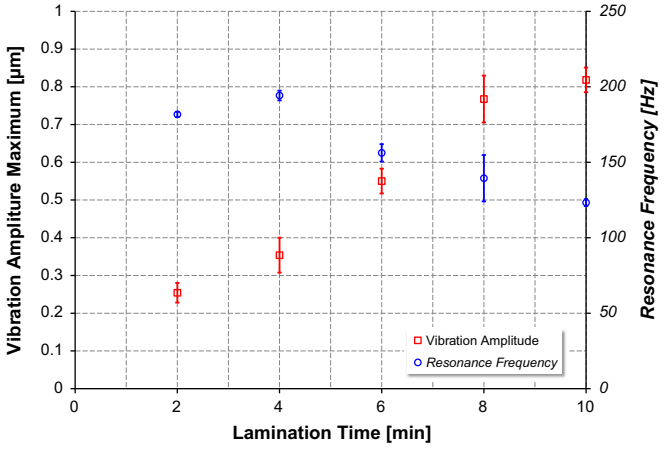

Fig. 17. Maximum vibration amplitude and resonance frequency vs. lamination time.

techniques relying on fundamentally different measurands, like the non-extractable gel content (Fig. 1, left), the number of formed crosslinks according as determined by Raman spectroscopy (Fig. 15) and the decrease in the amount of residual crosslinker as measured by IR spectroscopy (Fig. 13) yield similar results. For some of these effects, e.g. the discrepancies observed between the degrees of crosslinking as determined by the Soxhlet method and by DSC, plausible explanations exist; for others, further fundamental research concerning the interaction of the applied analytical methods and the EVA material will be needed to find the decisive factors for the discrepancies.

A third and final main finding is that the standard Soxhlet method proved to be a good and reliable, although time-consuming, reference method for the range of crosslinking typical for PV applications. The effect of the number of crosslinks between the polymer chains seems to play a minor role over most of the process window of PV-grade EVA. Only for (i) very short lamination times, where some of the polymer may still be soluble despite being already – weakly – crosslinked, and (ii) at long reaction times, when essentially all polymer chains are already crosslinked and the number of multiple crosslinks increases with increasing lamination times, some alternative methods analytically outperform the standard procedure.

4.2. *Off-line method development and materials research*

When regarding the choices for an easy-to-use analytical method for industrial process development in the PV industry pragmatically, the standardised *Soxhlet method* is likely to keep its role as the standard method of choice for the time being. Despite all its shortcomings, the method has two major advantages: (i) the analytical effort is low and (ii) the technique is absolute and calibration-free. Especially the latter is of major practical importance, as new materials can be characterised without requiring any prior knowledge regarding the material. In comparison, all other investigated methods require material-specific calibration functions to correlate the measurands to the degree of crosslinking, and/or some *ab-inito* knowledge of the specific material.

Coming closest to being a competitor to the standard method is probably *dynamic mechanical analysis*. In addition to being significantly faster than the Soxhlet method, the DMA yields direct information on the mechanical properties of the material. While being of obvious interest for a range of PV-related R&D tasks, the method requires substantial instrumental effort and suitably qualified operators. For a widespread industrial use, the unique selling proposition overcoming this could be an improved prediction – and hence optimisation – of the overall behaviour of the

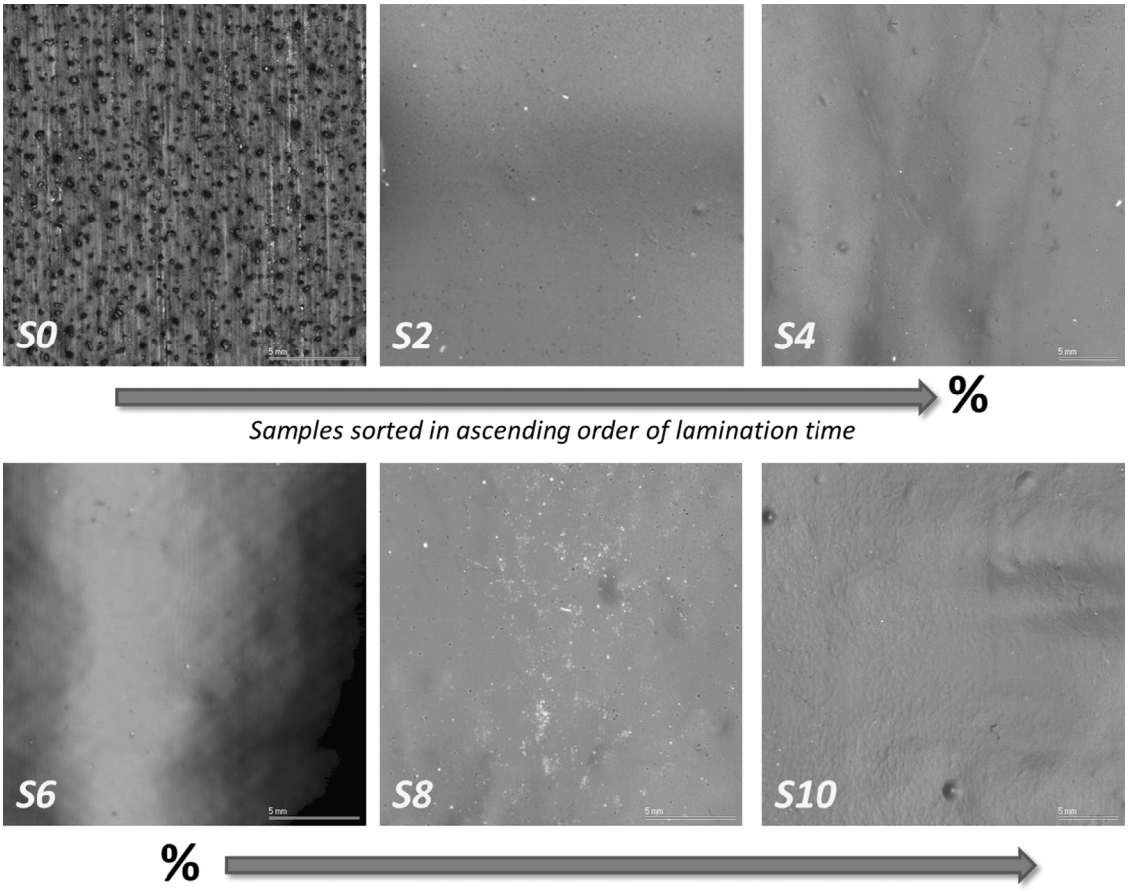

Fig. 18. SAM images of PV EVA samples on a polyamide backsheet, sorted by lamination time (0–10 min); fields of view: 30 × 30 mm².

Table 1
Comparative summary of the 17 investigated analytical approaches.

Method	Measurand	Analyte	Correlation Quality	In-line Applicability	Effort			Comments
					Instrumental	Qualification	Time	
Soxhlet Extraction	Gel content (mass loss)	Amount of non-extractable substance	(Reference method)	No	Low	Average	> 24 h	Calibration-free absolute method; harmful solvents involved
Solvent Swelling	Swellability (mass gain)	Solvent uptake	Good, but range-limited	No	Low	Average	~ 3 h	Harmful solvents involved; not applicable with weakly crosslinked EVA
Differential Scanning Calorimetry	Re-crystallisation enthalpy	Crystallinity	Poor	No	High	High	~ 1 h	
	Crosslinking reaction enthalpy	Residual amount of crosslinker	Good	No	High	high	~ 1 h	Indirect method requiring data on initial amount of crosslinker
Tensile Testing	Elastic modulus	Elastic characteristics	Uncorrelated	No	High	Average	< ½ h	
	Stress	Visco-elastic characteristics	Fair for lower degrees of crosslinking	No	High	Average	< ½ h	Method optimisation required
Shore Hardness	Hardness	Visco-elastic characteristics	Poor	(Potentially)	Average	Low	~1 min	PV cell damage observed in module tests; experimental re-design required
Dynamic Mechanical Analysis	Shear modulus ratio	Thermo-visco-elastic characteristics	Good	No	High	High	~1½ h	
	Damping factor	Thermo-visco-elastic characteristics	Good	No	High	High	~1½ h	
UV/Vis Spectroscopy	Transmission spectra	Opacity, crystallinity	Fair	Limited	Average	Average	< 1 min	In-line transmission spectroscopy limited to glass-glass modules
Mid-IR Spectroscopy	Transmission spectra	Residual amount of crosslinker	Good	No	High	average	~2min	Indirect method requiring data on initial amount of crosslinker

Table 1 (*continued*)

Method	Measurand	Analyte	Correlation Quality	In-line Applicability	Effort			Comments
					Instrumental	Qualification	Time	
	Attenuated total reflection spectra	Number of crosslinks formed	Fair	No	High	Average	~2 min	Relative method requiring data on initial material composition
Raman Spectroscopy	Raman spectra	Number of crosslinks formed	Good	Likely	High	Average	~1 min	Relative method requiring data on initial material composition
(Laser) Vibrometry	Resonance vibration of EVA	Elastic characteristics	Good	No	High	High	~5 min	Optimisation potential regarding effort
	Resonance vibration of module	Elastic characteristics	Uncorrelated	(Potentially)	High	High	~ ½ h	
Scanning Acoustic Microscopy	Acoustic impedance	Elastic characteristics	Uncorrelated	No	High	High	~10 min	Liquid US wave transmitter required

complete PV module over its full life-cycle, in comparison to what is possible from the gel content alone. The feasibility of this, however, has yet to be conclusively proven. The same applies to methods measuring the residual amount of crosslinker. While giving a reliable assessment of the crosslinking potential, the results are meaningful only in comparison to the initial amount of crosslinker present in the material before curing; the methods would thus require regular testing of the uncured material as reference. In addition, both pertinent methods (DSC and IR spectroscopy) involve extensive instrumentation and require qualified operators. All these methods are thus more of interest for R&D application than industrial everyday use.

4.3. Process control

The situation is significantly different when methods suitable for in-line process control are required. Being very much off-line, the standard Soxhlet method qualifies for quality control at best, but not for non-destructive on-line or even in-line use. In this study, only two optical methods showed realistic potential for measuring the degree of crosslinking of EVA encapsulants in-line in a PV manufacturing line: UV/Vis spectroscopy and Raman spectroscopy.

Instrumentally simple and easily implementable into a process environment, the correlation of UV/vis spectra of EVA elastomers on the degree of curing appears to depend primarily on light scattering. Still, this effect is rather weak and could be influenced also by the material composition and the processing conditions of the encapsulant sheets prior to lamination. The main practical concern, however, is the method's limitation to transmission measurements, i.e. glass–glass PV modules.

Altogether, *Raman spectroscopy* would appear the most promising approach for realising an in-line instrument for measuring the degree of EVA crosslinking in PV modules. The method is fast, non-destructive, easy to use (once a calibration model has been established), and requires only a single optically accessible side, i.e. the front glass. Moreover, cost-effective compact devices suitable for process integration are commercially available. Still, the method is relative, requiring either a highly reliably constant material composition, or regular testing of the uncured material to act as reference for the data evaluation. Further R&D will be required to establish this method, dealing in particular with the significance of the observed changes in the relative intensities of the methyl and methylene groups during crosslinking in comparison to other contributions to these spectral features. Possible interferences could be variations in the ethylene/vinyl acetate ratio as well as contributions by the various additives added to PV-grade EVA foils.

5. Outlook

This comparative method study established the availability of a range of different methods for use in off-line material analysis of PV-grade EVA encapsulants, allowing to measure the impact of the lamination process on a number of different application-relevant parameters. Some of these could yield an improved understanding of the curing process and its ramifications regarding EVA behaviour and PV module characteristics. Most likely, the different mechanical and thermo-mechanical methods, like DMA, will be of particular interest for this. Still, these investigations are only at their beginning; for instance, the customarily used requirement "$>$ 80% gel content after lamination" as a degree of crosslinking deemed "sufficient" appears to be based more on experience and tradition than on reliable technical and scientific data. This relates also to open questions regarding a possible post-curing continuation of crosslinking of the EVA in already installed PV modules, due to thermal cycling or/and photolytic activation by intense sunlight. To warrant the efforts needed for further method development and an eventual industrial implementation of new off-line methods, the logical next step is to ascertain what exactly can be learned from these measurands, and how that data could be used to improve the manufacturing and quality of PV modules.

While this is a demanding task involving a wide range of expertise and effort, the actual next steps will focus on validating a select few of the methods tested in this study using a wider sample range. This will involve attempting to replace the formerly used "lamination time" as correlation basis by either (i) the actual time at lamination temperature or by (ii) the thermal energy transferred into the EVA in the laminate stack. Moreover, the production of additional samples for intermediate lamination times, in particular in the highly dynamic curing region, is planned. Further investigations will address application-relevant practical issues, like the effect of using different EVA formulations and brands with deviating additives and crosslinking agents. Related to that, another R&D focus will attempt to identify the relevance of possible inhomogeneities in uncured EVA foils. Finally, a dedicated research project to develop Raman spectroscopy into an in-line analysis tool for determining the degree of crosslinking of EVA foils in PV modules is currently under preparation.

Acknowledgements

This investigation was performed as part of the K-Project IPOT (⟨http://www.ipot-project.at⟩) and co-funded within the R&D Program COMET—Competence Centers for Excellent Technologies by the Federal Ministries of Transport, Innovation and Technology (BMVIT) and Economics and Labour (BMWA), managed on their

behalf by the Austrian Research Promotion Agency (FFG). Additional financial support was provided by the Austrian Province of Carinthia.

IPOT project partner KIOTO Photovoltaics GmbH, and in particular Mr. Markus Spielberger, are gratefully acknowledged for the support in preparing the unified test sample set.

The DMA methodology was developed within the *Neue Energien 2020* project "PV Polymer" by the Polymer Competence Centre Leoben in cooperation with Perkin Elmer and the Chair of Materials Science and Testing of Plastics of the University of Leoben, and financially supported by the Austrian Klima-und Energiefonds (FFG no. 825379).

References

[1] A.W. Czanderna, F.J. Pern, Encapsulation of PV modules using ethylene vinyl acetate copolymer as a pottant: a critical review, Solar Energy Materials and Solar Cells 43 (2) (1996) 101–181, http://dx.doi.org/10.1016/0927-0248(95)00150-6.

[2] S. Kurtz, J. Wohlgemuth, T. Sample, M. Yamamichi, J. Amano, P. Hacke, M. Kempe, M. Kondo, T. Doi, K.Otani, Ensuring quality of PV modules, 37th IEEE Photovoltaic Specialists Conference (PVSC), : (2011) pp. 842–847 http://dx.doi.org/http://dx.doi.org/10.1109/PVSC.2011.6186084.

[3] S. Dietrich, M. Sander, M. Pander, M. Ebert, Interdependency of mechanical failure rate of encapsulated solar cells and module design parameters, Proceedings of SPIE 8472 article id. 84720P (online only), 9 pp. (2012) http://dx.doi.org/10.1117/12.9292893.

[4] Ch. Hirschl, M. Granitzer, L. Neumaier, M. Spielberger, W. Mühleisen, M. Kraft, G. Kroupa, J. Schicker, Combined Experimental and simulatory evaluation of thermal and mechanical loads on PV modules, 27th European Photovoltaic Solar Energy Conference, 2012 pp. 3561–3565 http://dx.doi.org/http://dx.doi.org/10.4229/27thEUPVSEC2012-4BV.3.55.

[5] P.R. Dluzneski, Peroxide Vulcanization of Elastomers, Rubber Chemistry and Technology 74 (3): 451-492 http://dx.doi.org/10.5254/1.3547647.

[6] S. Kajari-Schröder, U. Eitner, C. Oprisoni, T. Alshuth, M. Köntges, R. Brendel, Modelling the curing dynamics of ethylene-vinyl acetate, 25th European Photovoltaic Solar Energy Conference, 2010 pp. 4039–4043 doi: http://dx.doi.org/10.4229/25thEUPVSEC2010-4AV.3.25.

[7] R.F.M. Lange, Y. Luo, R. Polo, J. Zahnd, The lamination of (multi)crystalline and thin film based photovoltaic modules, Progress in Photovoltaics: Research and Applications 19 (2) (2011) 127–133 http://dx.doi.org/10.1002/pip.993.

[8] American Society for Testing and Materials, Standard Test Methods for Determination of Gel Content and Swell Ratio of Crosslinked Ethylene Plastics, ASTM D2765–11, 2006 http://dx.doi.org/http://dx.doi.org/10.1520/D2765-11.

[9] K. Agroui, A. Belghachi, G. Collins, J. Farenc, Quality control of EVA encapsulant in photovoltaic module process and outdoor exposure, Desalination 209 (1–3) (2007) 1–9, http://dx.doi.org/10.1016/j.desal.2007.04.001.

[10] Z. Xia, D. Cunningham, J. Wohlgemuth, A new method for measuring cross-link density in ethylene vinyl acetate-based encapsulant, Photovoltaics International 5 (2009) 150–159.

[11] M. Schubnell, Investigation of the curing reaction of EVA by DSC and DMA, Photovoltaics International 7 (2010) 131–137.

[12] W. Stark, M. Jaunich, Investigation of Ethylene/Vinyl Acetate Copolymer (EVA) by thermal analysis DSC and DMA, Polymer Testing 30 (2) (2011) 236–242, http://dx.doi.org/10.1016/j.polymertesting.2010.12.003.

[13] M. Hidalgo, F. Medlege, M. Vite, C. Corfias-Zuccalli, P. Voarino, J. Gonzalez-Leon, A new DSC method for the quality control of PV modules: simple and quick determination of the degree of crosslinking of EVA encapsulants, Photovoltaics International 14 (2011) 130–140.

[14] W. Mühleisen, M. Biebl-Rydlo, M. Spielberger, Determining the degree of EVA crosslinking in assembled PV modules acoustically and in-situ, 26th European Photovoltaic Solar Energy Conference, 2011 3480–3483, http://dx.doi.org/http://dx.doi.org/10.4229/26thEUPVSEC2011-4AV.1.59.

[15] H.Y. Li, L.E. Perret-Aebi, R. Théron, C. Ballif, Y. Luo, R.F. Lange, Optical transmission as a fast and non-destructive tool for determination of ethylene-co-vinyl acetate curing state in photovoltaic modules, Progress in Photovoltaics: Research and Applications 21 (2011) 187–194, http://dx.doi.org/10.1002/pip.1175.

[17] R.A. Mickiewicz, E. Cahill, P. Wu, Non-destructive determination of the degree of cross-linking of EVA solar module encapsulation Using DMA shear measurements, in: Proceedings of 38th IEEE Photovoltaic Specialists Conference (PVSC), 2012.

[18] P.J. Flory, Jr. Rehner, Statistical theory of chain configuration and physical properties of high polymers, Annals of the New York Academy of Sciences 44 (1943) 419–429, http://dx.doi.org/10.1111/j.1749-6632.1943.tb52762.x.

[19] G.W. Ehrenstein, G. Riedel, P. Trawiel, Thermal Analysis of Plastics, Hanser Verlag, München (D), 2004, p 163–217.

[20] International Organization for Standardization, Plastics – Differential scanning calorimetry (DSC) – Part 3: Determination of temperature and enthalpy of melting and crystallization, 2011, ISO 11357-3:2011.

[21] M. Pyda. (Ed.), "ATHAS Data Bank", ⟨http://athas.prz.rzeszow.pl⟩.

[22] M. Brogly, M. Nardin, J. Schultz, Effect of vinylacetate content on crystallinity and second-order transitions in ethylene-vinylacetate copolymers, Journal of Applied Polymer Science 64 (10) (1997) 1903–1912, http://dx.doi.org/10.1002/(SICI)1097-4628(19970606)64:10<1903::AID-APP4>3.0.CO;2-M.

[23] O. Bianchi, R.V. Oliveira, R. Fiorio, J. Martins, N. De, A.J. Zattera, L.B. Canto, Assessment of Avrami, Ozawa and Avrami–Ozawa equations for determination of EVA crosslinking kinetics from DSC measurements, Polymer Testing 27 (6) (2008) 722–729, http://dx.doi.org/10.1016/j.polymertesting.2008.05.003.

[24] International Organization for Standardization, Plastics – Determination of tensile properties – Part 3: Test conditions for films and sheets, 1995, ISO 527-3:1995.

[25] International Organization for Standardization, Rubber, vulcanized or thermoplastic – Determination of indentation hardness – Part 1: Durometer method (Shore hardness), 2010, ISO 7619-1:2010.

[26] P. Klemchuk, M. Ezrin, G. Lavigne, W. Holley, J. Galica, S. Agro, Investigation of the degradation and stabilization of EVA-based encapsulant in field-aged solar energy modules, Polymer Degradation and Stability 55 (3) (1997) 347–365, http://dx.doi.org/10.1016/S0141-3910(96)00162-0.

[27] C. Peike, T. Kaltenbach, K.A. Weiß, M. Koehl, Non-destructive degradation analysis of encapsulants in PV modules by Raman Spectroscopy, Solar Energy Materials and Solar Cells 95 (7) (2011) 1686–1693, http://dx.doi.org/10.1016/j.solmat.2011.01.030.

[28] C. Peike, T. Kaltenbach, K.A. Weiß, M. Koehl, Indoor vs. outdoor aging: polymer degradation in PV modules investigated by Raman spectroscopy, Proceedings of SPIE 8472: 84720V (2012) http://dx.doi.org/10.1117/12.929828.

[29] L. Neumaier, W. Mühleisen, A. Kenda, Ch. Hirschl, Charakterisierung von Photovoltaik-Modullaminaten mittels Vibrometermessungen, Proceedings of the Solarsymposium Bad Schaffelstein 2013, p 167–177 In press.

[30] L. Woo, M.T. Ling, S.P. Westphal, Dynamic mechanical studies on secondary relaxations of ethylene copolymers, Thermochimica Acta 243 (2) (1994) 147–154, http://dx.doi.org/10.1016/0040-6031(94)85049-6.

[31] R. Androsch, Melting and crystallization of poly(ethylene-co-octene) measured by modulated d.s.c. and temperature-resolved X-ray diffraction, Polymer 40 (10) (1999) 2805–2812, http://dx.doi.org/10.1016/S0032-3861(98)00470-4.

[32] S.H. Schulze, C. Ehrich, I. Hinz, M. Schak, "Crosslinking of EVA copolymers by thermal and radiation curing processes", Plastics in Photovoltaics 2012 conference, Phoenix/Arizona (2012).